Electrical Power and Energy Systems 24 (2002) 113–120

ELECTRICAL POWER & ENERGY SYSTEMS

www.elsevier.com/locate/ijepes

Dynamic equivalent of external power system and its parameter estimation through artificial neural networks

A.H.M.A. Rahim[a,*], A.J. Al-Ramadhan[b]

[a]Department of Electrical Engineering, K.F. University of Petroleum and Minerals, Dhahran, Saudi Arabia
[b]Southern Area Operation Engineering, Saudi Arabian Oil Co., Dhahran, Saudi Arabia

Received 25 May 1999; revised 3 January 2001; accepted 2 February 2001

Abstract

A multi-machine power network, external to a study system, has been replaced by one equivalent machine for dynamic studies. The back-propagation and radial-basis function neural networks have been employed to estimate unknown parameters of the dynamic equivalent. Transient stability indices like the peak overshoot, decay constant and frequency of oscillations of the study generator are used as input features to train the neural networks. While the back-propagation algorithm, generally, did not give very satisfactory estimates, the radial basis functions could be trained to predict the parameters of the equivalent with extreme precision. Estimating the dynamic equivalent from the transient stability indices is a novel approach. © 2002 Elsevier Science Ltd. All rights reserved.

Keywords: Dynamic Equivalent; Aggregation; Artificial Neural Network

1. Introduction

Assessment of dynamic performance of a modern power system is a complex procedure because of very large number of generating units and their associated control elements in it. Because of load growth, the system sizes are ever growing. Addition of a new plant requires, in turn, a large number of planning studies. The dynamic study is one of the very complicated analyses requiring solution of hundreds of differential equations. However, when a new component is added to the system, if the existing system can be replaced dynamically by one or more suitable equivalents, a tremendous amount of computation can be saved.

Efforts to find a suitable equivalent of the power system, which could faithfully approximate its dynamic behavior, have been reported since the 70s [1,2]. Usually, the system to be equivalenced is replaced by one or more coherent groups of synchronous machines. Dynamic equivalents using frequency response and modal coherency [3], angular speed deviation based coherency [4], acceleration and velocity-based coherency [5], and energy function and rotor angle based coherency analysis [6], etc. has been reported in the literature. Dynamic equivalent of non-coherent groups, or equivalent of several coherent groups is usually more difficult to determine. The system external to the local or study machine may be represented by an equivalent synchronous motor with unknown parameters. Identification and parameter estimation techniques have been employed to determine these unknown parameters [7,8]. The grid system has also been represented by an equivalent synchronous generator with its own controllable components [9].

Besides the computational requirements of the iterative methods based on least square techniques to estimate the parameters, one serious disadvantage of these methods is that the convergence of the solutions are not guaranteed. The desired solutions can be arrived at only if the initial guess is reasonably close. Also, not all the parameters may converge simultaneously [8]. An alternative to the weighted least square technique based estimation procedure is the application of artificial neural networks (ANN). Since the dynamic behavior of the system is of interest, matching the electromechanical and electrical transient time response with the parameters of the unknown equivalent, as such, may be a formidable task.

In this work, proper input features of the study system, which reflect the dynamic performances of the equivalent, are extracted from the local system. Transient stability indices like peak overshoot, decay constant, natural frequency of oscillation, etc. are utilized to predict the inertia constant, the reactances and other parameters of the equivalent machine. Two ANN — the back-propagation

* Corresponding author. Tel.: +9663-860-2277; fax: +9663-860-3535.
E-mail address: ahrahim@kfupm.edu.sa (A.H.M.A. Rahim).

PII: S0142-0615(01)00016-3

(BP) and radial-basis function (RBF) — have been trained. Using the selected transient stability indices as inputs, the RBF network was observed to predict the parameters very precisely. The authors in Ref. [10] reported the initial work.

2. The power system model

The power system model comprises of a known (local) system connected to a large interconnected network through a transmission system. The local system also has its own load lumped at its generator bus. Viewed from this system, the rest of the grid behaves like a huge load operating at synchronous frequency. This can be represented by a synchronous motor with unknown parameters. The configuration of the local system connected to the grid (external) system, represented by the synchronous motor, is shown in Fig. 1.

A relatively detailed model of the local generator has been considered. It includes the electromechanical swing equation, field flux decay equation, and the IEEE type 4 ST exciter model. Because the short duration dynamic performance is of interest, the governor model has not been included. The state variables chosen are the generator speed deviation, rotor angle and internal voltage of the machine, and the exciter voltage. The dynamic equation can be written in the form

$$\dot{x}_i = f_i[x_i, v_0, u_i] \tag{1}$$

where u_i is the vector of controls for the local system and V_0 the terminal voltage of the equivalent machine.

Since the internal behavior of the equivalent motor is not of interest, it is modeled by a third order model, which includes the electromechanical swing equation and the field flux decay. Thus, the states are the motor speed deviation, rotor angular position and the internal voltage of the equivalent motor. The unknown equivalent (j) is then represented in the form

$$\dot{x}_j = f_j[x_j, v_t, \gamma] \tag{2}$$

where, α is the vector of unknown parameters through which the equivalent motor is characterized. These are the inertia constant (M), damping coefficient (D), direct axis synchronous reactance (x_d), direct axis transient reactance (x'_d) and the open circuit field time constant (T'_{do}) of the motor. v_t is the terminal voltage of the study system. Expressing v_t and v_0 in terms of the seven state variables selected, the composite state model for the system is expressed as

$$\dot{x} = f[x, \alpha, \gamma] \tag{3}$$

The steps in the derivation of the state model are given in Appendix A.1.

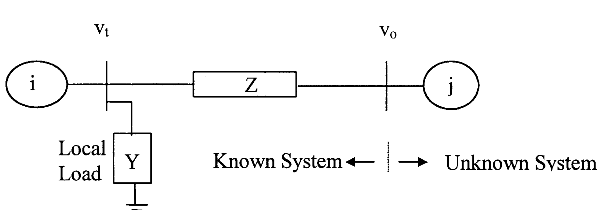

Fig. 1. The power system configuration.

3. The artificial neural networks

ANNs have been used widely in power system applications in recent years [11]. A great deal of work has been carried out on dynamic security analysis, particularly in the determination of fault clearing times [12–14]. The theory is widely available in the literature and is outlined here, in brief, to show the various steps involved in the computational procedure.

3.1. The back-propagation network

Fig. 2 shows the layout of a back-propagation network with a three-layer perceptron — the input, the hidden and the output layers having activation functions in the hidden and output layers. The number of neurons in these layers is assumed to be p, r and m, respectively. The training starts by arbitrarily assuming a weighting function w_{ji}, which relates the input and output of hidden neuron j at any iteration n as follows [15].

$$v_j(n) = \sum_{i=0}^{p} w_{ji}(n)x_i(n) \qquad y_j(n) = \varphi_j(v_j(n)) \tag{4}$$

where x_i are the input data and w_{j0} corresponds to the fixed input $x_0 = -1$ and is the threshold applied to neuron j. φ is a logistic activation function of the sigmoid type. For neuron k at the output layer, the net internal activity level is

$$v_k(n) = \sum_{j=1}^{r} w_{kj}(n)y_j(n) \tag{5}$$

The error signal at the output node k is defined as the difference between the desired output d and the actual output y. The activation function φ_k at the output neuron usually is of linear type.

In the training process, the network is presented with a pair of patterns — an input pattern and a corresponding desired output pattern. In the back-propagation algorithm, there are two distinct passes of computation. In the forward

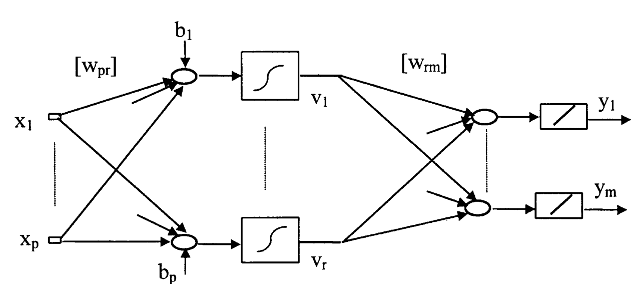

Fig. 2. The back-propagation neural net configuration.

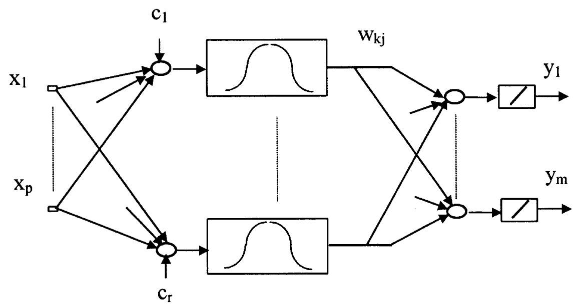

Fig. 3. Radial-basis function net configuration.

pass, the outputs are computed on the basis of selected weights and the error is computed. In the backward pass, the weights are updated so as to minimize the sum of the squares of errors. The synaptic weight w_{ji} at any layer l is updated through the steepest descent technique. The solution is accelerated through a proper choice of momentum constant α and learning rate parameter η and is finally expressed as

$$w_{ji}(n+1) = w_{ji}(n) + \alpha[w_{ji}(n) - w_{ji}(n-1)] + \eta\delta_j(n)y_i^{l-1}(n) \quad (6)$$

where

$$\delta_j(n) = \varphi'(v_j(n))\sum_k \delta_k^{i+1}(n)w_{kj}^{l+1}(n). \quad (7)$$

3.2. The radial-basis function network

Fig. 3 shows the general structure of a neural network, which employs the RBF. The input output relationship of a general RBF network with p inputs, **r**-hidden nodes and m outputs is expressed as

$$y_j = \sum_{k=1}^{r} w_{kj} g(\|(x - c_k)\|, \sigma_k) \quad (8)$$

where, w_{kj} are the set of adjustable weights for the kth node's contribution to the jth output. c_k and σ_k ($k = 1,2,\ldots r$) represent the center and width, respectively, of the basis or activation function. The basis function is usually taken to be having a Gaussian distribution as shown in the figure. In training the RBF network, the centers and the width need adjusting. The linear weights w_{kj} in Eq. (8) are estimated so as to minimize the sum of the square of the error between the desired output $d(k)$ and the network output $y(k)$, where the error is

$$e(k) = d(k) - y(k), \qquad k = 1,2,\ldots m. \quad (9)$$

An orthogonal least squares (OLS) procedure proposed by Chen [16] chooses the centers of the radial basis functions as subsets of the weighting matrix from a linear regression model of the error equation, and is written in matrix form as

$$d = Xa + e \quad (10)$$

where d is the vector of desired response, a the model parameter matrix, X is the regressor and e the residue. Through an orthogonalization procedure it is shown that [15],

$$w_1 = x_1 \quad (11)$$

$$\alpha_{ik} = (u_i^T X_k)/(u_i^T u_k) \qquad 1 \le i \le k$$

$$w_k = x_k - \sum_{i=1}^{k-1} \alpha_{ik} x_i$$

where $k = 2,3,\ldots r$.

The training vector w_1, w_2,…, which include the centers are determined in a well-defined manner until the procedure is terminated at the sth step when

$$1 - \sum_{j=1}^{s} [\mathrm{err}]_j < \rho \quad (12)$$

Here, $0 < \rho < 1$ is a chosen tolerance, and the error at the nth step is computed as

$$\max_n \{((W_k^T d/W_k^T W_k)^2 W_k^T W_k)/d^T d\}; \qquad k = 1,2,\ldots r. \quad (13)$$

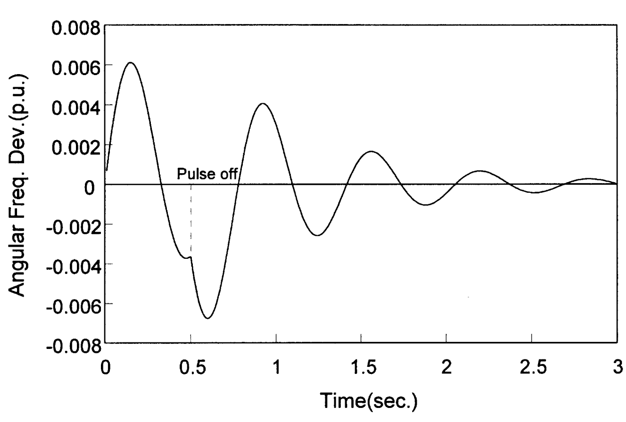

Fig. 4. Angular speed deviation of local generator following a 35% input torque pulse for 0.5 s.

4. Generation of training data for ANN

Both the back-propagation and radial-basis function neural networks presented above were employed to estimate the unknown parameters γ given in Eq. (3). Input features, which reflect the behavior of the parameters, have to be properly selected to train the networks. It is expected that the effect of parameters M (inertia) and D (damping) of the equivalent external machine will be embedded in the electromechanical transients of the study system as depicted in the variation of its angular frequency. Similarly, x'_d and T'_{do} can be assessed from the variation of terminal voltage transients. The input features that were considered to train the neural nets are the peak overshoot, decay coefficient, frequency of natural oscillation of angular frequency and

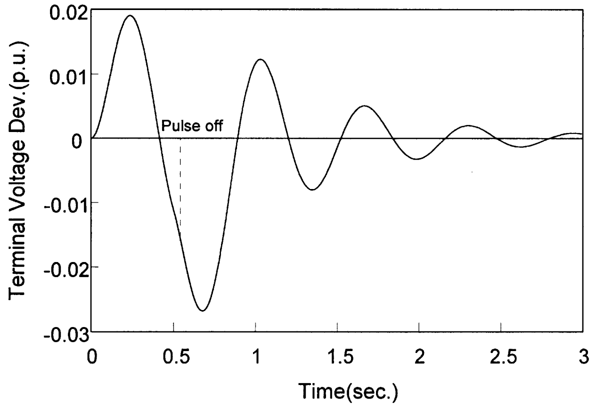

Fig. 5. Terminal-voltage variation of the local generator for the disturbance condition of Fig. 4.

the terminal voltage variations of the local system. The steady state power flow will be affected by the synchronous reactance x_d of the equivalent motor. So, this is also included in the input features.

To generate input–output data to train the neural nets, disturbances are simulated on the local system and the transients are recorded. For a 35% input torque pulse for 0.5 second on the local generator, sample plots for the rotor speed deviation and the terminal voltage variations are given in Figs. 4 and 5. A total of 100 simulations were made for the system given in Fig. 1 representing equivalence of different power systems. From the transient records the following data has been collected.

- Peak overshoot, decay coefficient, and natural frequency of oscillations of the electromechanical transients as exhibited by rotor angular frequency deviation.
- The same indices for electrical transients obtained from change in terminal voltage.
- The steady state power flow between the local and external systems.

System parameters and the nominal operating conditions are given in Appendix A.2.

The procedure for generation of test data is summarized in the following.

1. Select a set of acceptable values of parameters M, D, T'_{do}, x'_d and x_d for the equivalent external system. These form the output data set in the ANN test procedure.
2. For the given parameters of the local system and for a particular loading, calculate all the operating quantities, including the system voltages and power flow, for both the local and test systems.
3. For a transient disturbance on the local system solve the system dynamic Eq. (3) for the composite system, and record angular frequency and terminal voltage variations $\Delta\omega$ and Δv_t, respectively.
4. From the record of $\Delta\omega$ and Δv_t find the peak overshoot, decay constant and period of oscillations of both the electromechanical and electrical transients. These 6 quantities, in addition to the steady state power flow, form the input data set corresponding to the output values of step 1.
5. Repeat steps 1–4 for the required number of data sets.

5. Results

Following the procedure outlined in the previous section, a total of 100 simulations were run. Amongst the 100 data sets generated, 80 samples were used to train the nets and the other 20 to test them. The selection was done randomly. Several combinations of test-train sets were attempted. Though the selections for the test and train sets were

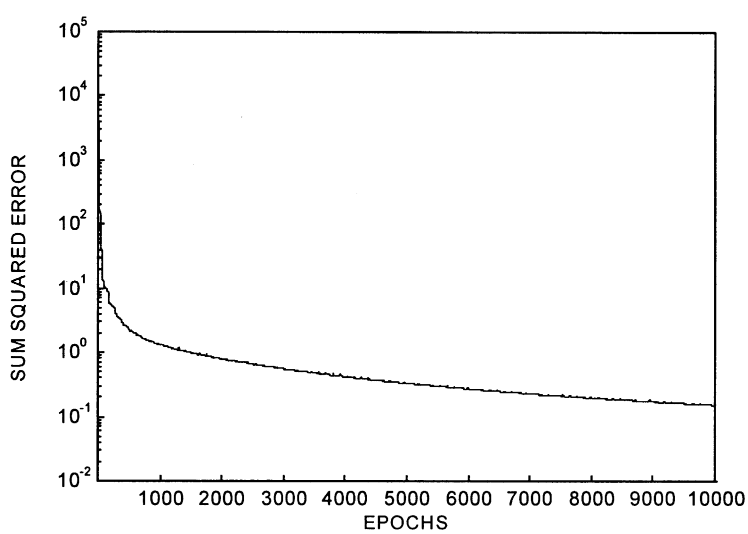

Fig. 6. Training error convergence characteristics for the back-propagation network.

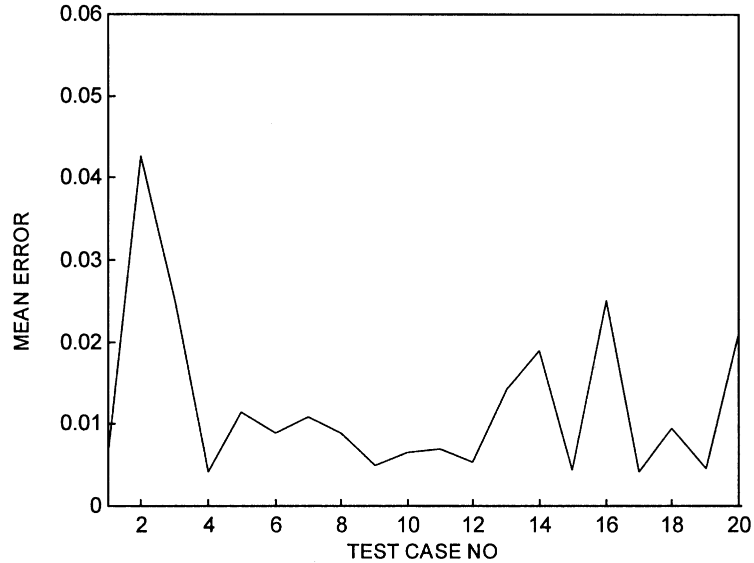

Fig. 7. Mean error for the randomly selected test samples.

random, care has to be taken so that the net is presented with a broad range of data in the training phase.

The convergence characteristics of the training error from the back-propagation network are shown in Fig. 6. The sum-squared error converged to 0.1 approximately, after about 10,000 presentations with 100 neurons in the hidden layer. This is almost the optimum number in terms of error convergence for all the cases considered. The values used for learning rate (η) and momentum constant (α) in Eq. (6) were 0.01 and 0.9, respectively. The error ratio used was 1.04, and ratios for increasing and decreasing the learning rates were 1.05 and 0.7, respectively. The trained network was then tested on the randomly selected data samples. The mean error between the actual and network estimated values for the 5 outputs calculated through relationship (14) is shown in Fig. 7. The output variables are not normalized.

$$\text{Mean error} = \frac{1}{5}\sqrt{\sum_{k=1}^{5}(e_k^2)} \tag{14}$$

As can be observed from Fig. 7 the maximum error is about 0.04 for sampling #2 which does not appear to be too bad. Since the output contains quantities like inertia constant (range 2–15), transient reactance (range 0.1–0.3), the mean error fails to show the level of convergence of these smaller quantities. Comparison of the actual values and the estimated ones from the BP algorithms for reactances x_d and x'_d are shown in Figs. 8 and 9, respectively.

Contrary to the BP algorithm, the RBF network can be trained to almost any level of accuracy. Since higher

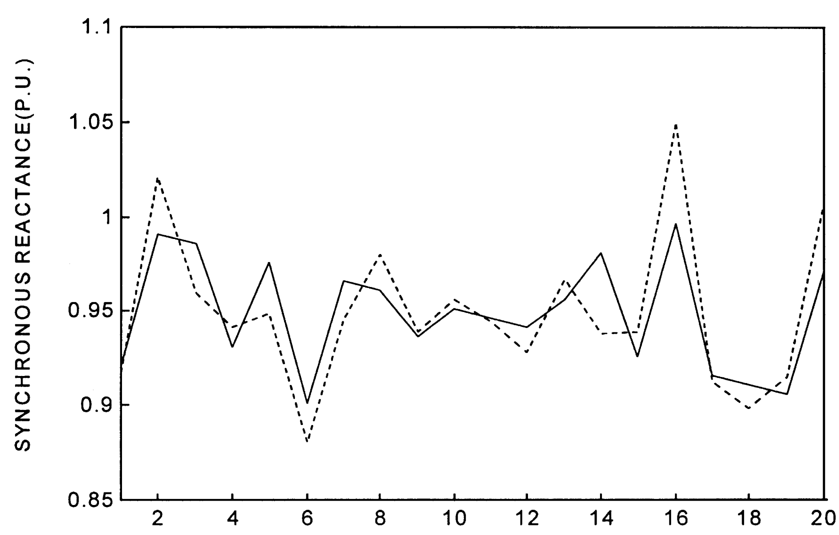

Fig. 8. Comparison of the values of synchronous reactance x_d, — actual, – – – back-propagation net estimates.

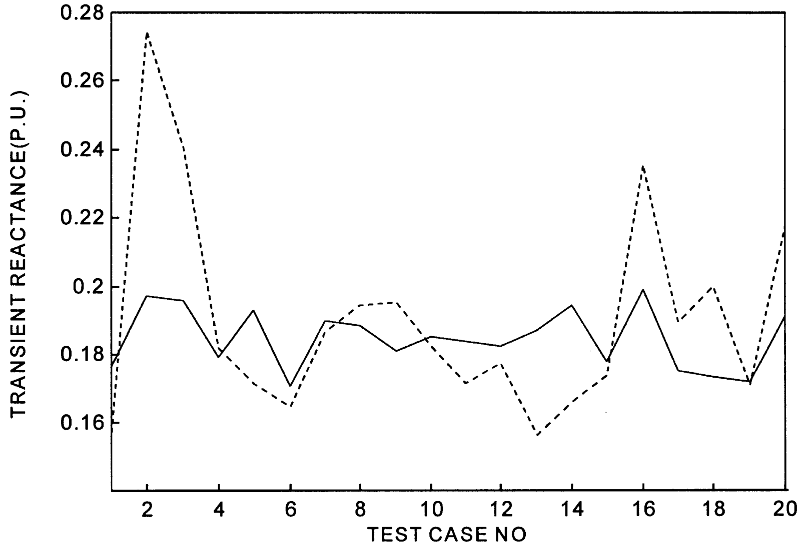

Fig. 9. The comparison of transient reactance x'_d. Symbols are as in Fig. 8.

accuracy involves excessively large number of neurons in the hidden layer, care should be taken that there is no overfitting of data in which case the training becomes useless. Also the width of the basis functions has to be properly selected to get a good match. For an error convergence limit of 10^{-3} and the width of the basis function of 0.01, Fig. 10 shows the convergence characteristics of the training error for the RBF network. It can be observed that the RBF network needs only 26 neurons in the hidden layer in the training phase. The computation time is of the order of seconds compared to that of hours in the back-propagation network. The mean error for the test samples obtained through the RBF network and as calculated in Eq. (14) is shown in Fig. 11. The mean error for the test samples is of the order of 10^{-3}, which is extremely small.

Fig. 12 gives a plot of the largest parameter, M as obtained through the RBF network. The predicted values are so close to the actual values that they are indistinguishable on the plot. As stated, the parameter values are not normalized and so are the error terms in Fig. 10. The error convergence characteristics of the other parameters, D, T'_{do}, x'_d, x_d are equally good.

6. Conclusions

A power network is represented dynamically by a synchronous motor with unknown parameters. Transient stability indices of the study system were selected as input features for training the back-propagation and RBF neural

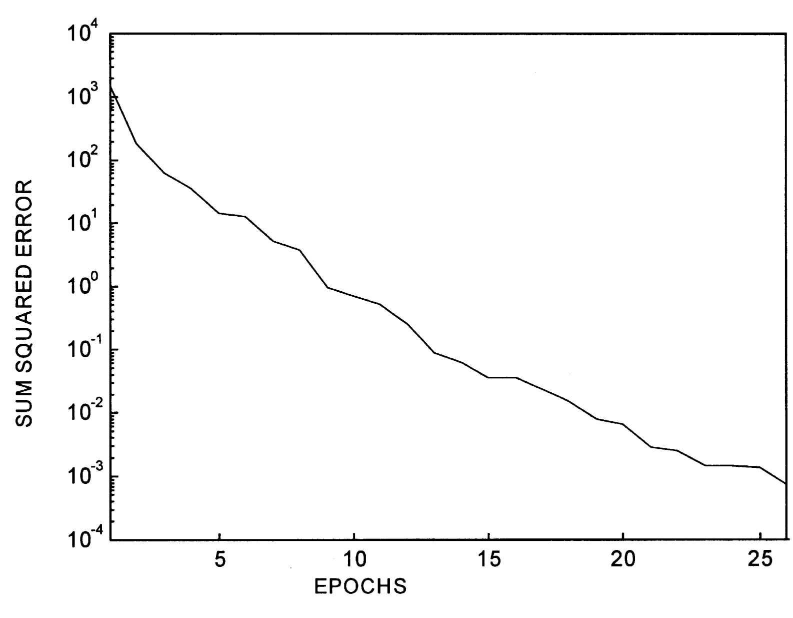

Fig. 10. Training error convergence characteristics for RBF network.

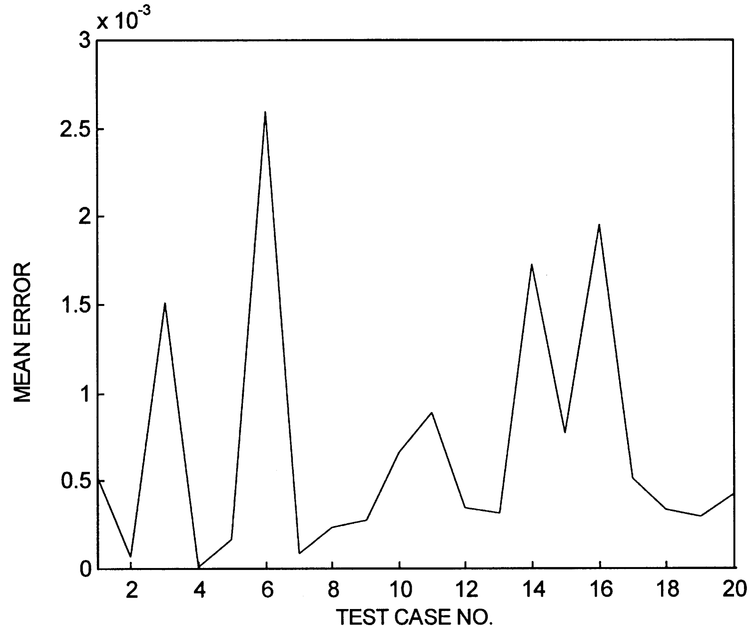

Fig. 11. Mean error with the RBF net for the randomly selected test cases.

networks to predict the unknown parameters of the system. It was observed that the RBF network could be trained with extreme precision for the selected input features. Training a network with transient stability indices like peak response, decay constant, etc., to estimate the dynamic equivalence of a power system is a novel idea.

Classical parameter estimation methods, generally, employ linearized system model, which depend on system operating conditions. Estimates obtained from a linearized model may require refinements or updates when the operating conditions change. The advantage of this estimation procedure through neural network is that system nonlinearities are retained in the generation of input–output data. Also, the nets are trained for a variety of operating conditions and a variety of disturbances. Since the equivalent power system is modeled through only five parameters, the volume of data to be handled by the nets will not be excessive in actual implementation.

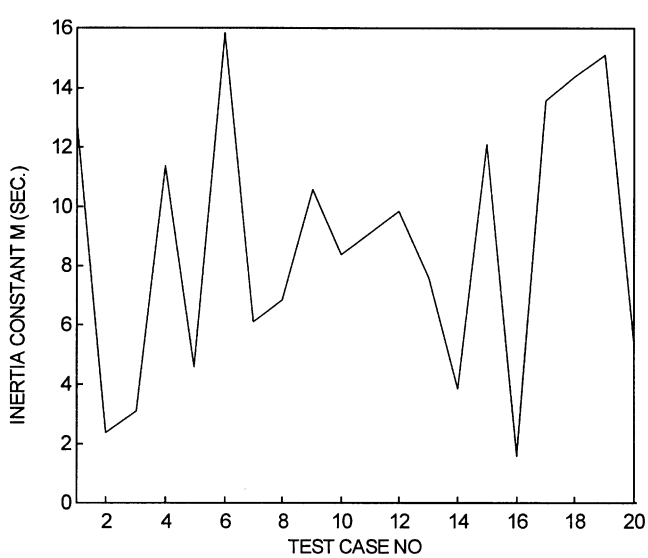

Fig. 12. Inertia constant M obtained through the RBF network for various test cases (the actual values overlapping with the predicted ones).

Acknowledgements

The authors wish to acknowledge the facilities provided towards this research at the King Fahad University of Petroleum and Minerals, Dhahran, Saudi Arabia.

Appendix A

A.1. The dynamic model

Referring to the notations in Fig. 1, the equation for the transmission line including the local load is

$$ZI_i = (1 + ZY)v_t - v_0 \tag{A1}$$

Representing the quantities along the direct and quadrature axes components as

$$I_i = I_{di} + jI_{qi} \quad v_t = v_{di} + jv_{qi} \quad v_0 = v_0 \sin \delta_I + jv_0 \cos \delta_I \tag{A2}$$

$$v_{di} = x_{qi}I_{qi} \quad v_{qi} = E'_{qi} - x_{di}I_{di} \tag{A3}$$

and solving simultaneously for I_{di} and I_{qi} in terms of the state variables as

$$I_{di} = g_1[E'_{qi}, \delta_I, v_0] \;\; I_{qi} = g_2[E'_{qi}, \delta_I, v_0] \tag{A4}$$

the terminal voltage can be expressed as follows.

$$v_t = \sqrt{v_d^2 + v_q^2} = g_3[E'_{qi}, \delta_I, v_0] \tag{A5}$$

The torque equation is

$$M_I \ddot{\delta}_i + D_I \delta_i = T_{mi} - T_{ei} \tag{A6}$$

where

$$T_{ei} = v_{di} I_{di} + v_{qi} I_{qi} \tag{A7}$$

The generator internal voltage equation is

$$\dot{E}'_{qi} = [E_{fdi} - (x_\mathrm{d} - x'_\mathrm{d}) I_{di} - E'_{qi}]/T'_{qoi} \tag{A8}$$

The exciter equation is

$$\dot{E}_{fdi} = \frac{K_i}{T_i}[v_\mathrm{t} - v_\mathrm{tr}] + \frac{1}{T_r} E_{fdo} \tag{A9}$$

Substituting the expressions for T_{ei}, v_t, I_{di}, etc., Eqs. (A6), (A8) and (A9) give the dynamic model (1) for the local study system.

The transmission line equation is

$$ZI_j = v_\mathrm{t} - v_0 \tag{A10}$$

where

$$I_j = I_{dj} + jI_{qj} \;\; v_t = v_{dj} + jv_{qj} \;\; v_0 = v_{0dj} + jv_{0qj} \tag{A11}$$

Also, $v_0 = -v_0 \sin \psi_j + jv_0 \cos \psi_j$, ψj is the angle between v_0 and q_j axes.

$$v_{0dj} = -x_j I_{qj} \;\; v_{0qj} = E'_{qj} + x_j I_{dj} \tag{A12}$$

The torque equation is

$$M_j \ddot{\delta}_j + D_I \dot{\delta}_j = T_{mj} - T_{ej} \tag{A13}$$

where, $T_{ej} = v_{dj} I_{dj} + v_{qj} I_{qj}$

Note here that δ_i is the angle between v_0 and q_i axis, while δ_j is the angle between v_t and q_j axes.

The internal voltage equation for the motor is

$$\dot{E}'_{qj} = [E_{fdj} - (x_\mathrm{d} - x'_\mathrm{d}) I_{dj} - E'_{qj}]/T'_{qoj} \tag{A14}$$

Substituting the appropriate relations, Eqs. (A13) and (A14) give the dynamic model (2) for the external equivalent system.

A.2. System parameters

The parameter values and nominal loading of the local system

M5 s	D 10 pu	x_d1 pu	x'_d 0.1 pu
x_q0.6	T'_do7.8 s	K_r50 pu	T_r 0.05 s

Local load	$G0 = 0.5$ at 0.9 pf lagging.
Local generator	$P_\mathrm{e} = 0.9$;$v_\mathrm{t} = 1.05$; pf = 0.9 lagging
Intertie	$Z = (0.04 + j0.5)$ pu

Parameters of the unknown system for the test case

M9.261 s	D25.91 pu	x_d0.5765 pu	x'_d 0.414 pu
T_{do}5.273 pu			

References

[1] Debs AS. Estimation of external network equivalents from internal system data. IEEE Trans Power Appl Syst 1975;94:273–9.
[2] Podmore R. Identification of coherent generators for dynamic equivalents. IEEE Trans Power Appl Syst 1978;97:1344–54.
[3] Van Oirsouw PM. Dynamic equivalents using modal coherency and frequency response. IEEE Trans Power Syst 1990;5(1):289–95.
[4] Pires de Souza EJS. An efficient methodology for coherency based dynamic equivalents. IEEE Proc — C 1992;139(5):371–82.
[5] Hussain MY, RauVG. Coherency identification and construction of dynamic equivalent for large power system. IEE Second International Conference on Advances in Power System Control, Operation and Management, Hong Kong, 1993. pp. 887–92.
[6] Haque MH, Rahim AHMA. Identification of coherent generators using energy function. IEE Proc — C 1990;137(4):255–60.
[7] Yu Y, El-Sharkawi MA, Yvong MA. Estimation of unknown large power system dynamics. IEEE Trans Power Appl Syst 1979;98:279–89.
[8] Rahim AHMA, Al-Baiyat IA. A weighted least squares method for determination of power system equivalents. Electric Power Syst Res 1982;5:207–18.
[9] Noorozian M, Andersson G. Damping of power system oscillations by use of controllable components. IEEE Trans Power Deliv 1994;9(4):2046–54.
[10] Rahim AHMA, Al-Ramadhan AJ. Parameter Estimation of Power System Dynamic Equivalents Using ANN, Summer Computer Simulation Conference'99, Chicago, July, 1999.
[11] Dillon T, Niebur D. Neural net application in power systems. Leics, UK: CRL Publishing, 1995.
[12] Sobajic D, Pao YH. Artificial neural network based dynamic security assessment of electric power systems. IEEE Trans Power Syst 1989;4(4):220–8.
[13] Pao YH, Sobajic DJ. Combined use of unsupervised and supervised learning for dynamic security assessment. IEEE Trans PWRS 1992;7(2):787–884.
[14] Moechtar M. Combination of Neural Network and Genetic Algorithm Methods for Assessing the Transient Stability of Power Systems, PhD Dissertation, University of Southern California, 1996.
[15] Haykin S. Neural networks. New York: Macmillan, 1994.
[16] Chen S, Cowan CFM, Grant PM. Orthogonal least squares learning algorithm for radial basis function networks. IEEE Trans Neural Networks 1991;2(2):302–9.